Journal of Inorganic Biochemistry 193 (2019) 1–8

Contents lists available at ScienceDirect

Journal of Inorganic Biochemistry

journal homepage: www.elsevier.com/locate/jinorgbio

Synthesis, anticancer activity and mechanism of iron chelator derived from 2,6-diacetylpyridine bis(acylhydrazones)

Qian Yao[a,1], Jinxu Qi[a,b,1], Yunyun Zheng[b], Kun Qian[a], Lai Wei[a], Mukedasi Maimaitiyiming[a], Zhen Cheng[c], Yihong Wang[a,*]

[a] School of Chemistry and Chemical Engineering, Southeast University, Nanjing 211189, China
[b] Medical School of Pingdingshan University, Pingdingshan 467000, China
[c] Stanford Cancer Institute, Member of Academic Council, Stanford University, USA

ARTICLE INFO

Keywords:
Chelator
Anticancer activity
Reactive oxygen species
Cell cycle
Apoptosis

ABSTRACT

We synthesized five iron chelator derived from 2,6-diacetylpyridine bis(acylhydrazones) and proved their iron complexes structure by X–ray single crystal diffraction. These ligands have a significant anticancer proliferative activity and low cytotoxicity against normal cells. The Fe(III) complexes show reduced cytotoxic activity compared to the metal–free ligands. Anticancer mechanism studies indicate that ligands with a potential anticancer proliferation activity by inhibiting the activity of ribonucleotide reductase. Ligand rather than iron complexes regulate the expression of cell cycle associated proteins and inhibit cell cycle arrest in S phase. Apoptosis mechanism results showed that both ligand and iron complexes did not significantly promote apoptosis.

1. Introduction

Iron is not only an important player in the DNA synthesis, oxidative phosphorylation process and replication activities of cells, but also regulates tumorigenesis related genes through hypoxia–inducible factors [1–3]. Especially, neoplastic cells are more sensitive than normal cells to iron, which may be because cancer cells express higher iron containing enzymes, ribonucleotide reductase (RR) [4,5]. Compared with normal cells, tumor cells proliferate faster and have a higher ability to express RR, which makes this enzyme a suitable target for cancer chemotherapy [6–8].

Ribonucleotide reductase is the only enzyme that catalyzes the reduction of ribonucleotides to produce the corresponding deoxyribonucleotides, which is a key enzyme and rate limiting enzyme for DNA synthesis and repair, and plays a regulatory role in cell proliferation and differentiation [7]. This enzyme is an important target for studying DNA synthesis and repair, cell proliferation and differentiation, as well as cancer treatment and anticancer drug development [8–11]. RR catalyzes the production of a stable lysyl radical by combining the oxygen with the Fe—O—Fe structure in the R2 subunit [12,13]. The metal chelator binds to iron in the R2 subunit to inhibit the activity of RR and cell proliferation [9]. After half a century of research, a series of metal chelators have been used in phase I and phase II clinical trials [3,14–16]. Thiosemicarbazone and acylhydrazones chelating agents have higher inhibitory activity against RR than others [17–20].

With the deepening of research, scientists have found that semicarbazide and acylhydrazones have wider applications, such as antibacterial, antitumor, anti–leukemia, etc. [21–26]. Isoniazid was invented in 1952, which made a fundamental change in the treatment of tuberculosis [27–29]. In this nearly 60–year history of use, although some patients infected with tuberculosis have developed resistance, most doctors still consider it an indispensable drug for the treatment of tuberculosis [30–32]. 2–Pyrrolylcarboxyisopropyl hydrazine (HPCIH), a Fe chelator, effectively prevents cells uptaking iron from the iron transporter transferrin (Tf) [3,33]. The NNO or ONO structure characteristic of the acylhydrazone chelator makes it form a stable complex with iron, which deactivates the ferritin–containing enzyme [34]. Recent studies have shown that the lipophilicity and membrane permeability of acylhydrazones analogues play a key role in the chelation of Fe [35–38].

In order to develop a new type of chelating agent with high iron mobilization effect to resist tumor proliferation, we synthesized the 2,6-diacetylpyridine bis(acylhydrazones) series in this study. In order to obtain better iron activation and anticancer proliferative activity, we designed these ligands containing bis-semicarbazide. We selected three

* Corresponding author at: 2 Southeast Road, Nanjing 211189, China.
E-mail address: yihongwang@seu.edu.cn (Y. Wang).
[1] Qian Yao and Jinxu Qi equally contributed to this study.

https://doi.org/10.1016/j.jinorgbio.2019.01.003
Received 6 November 2018; Received in revised form 1 January 2019; Accepted 7 January 2019
Available online 10 January 2019
0162-0134/

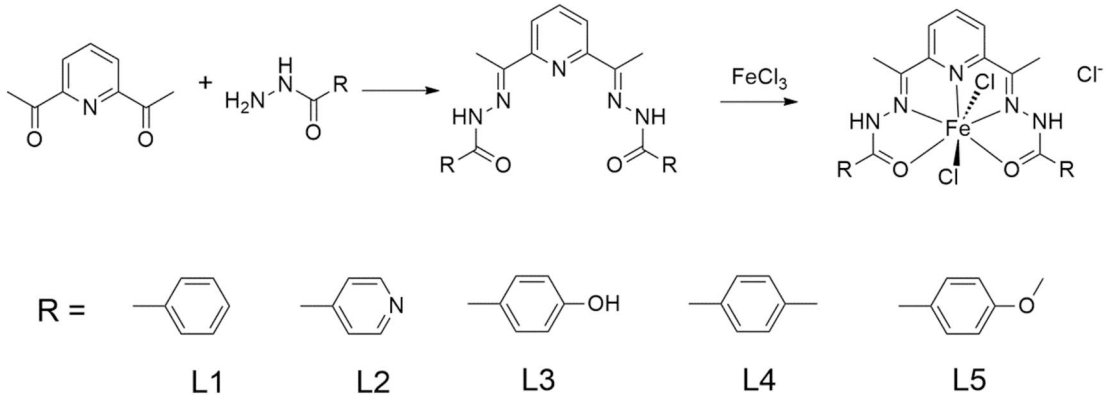

Scheme 1. Synthesis routes for ligands (L1–L5) and Fe complexes.

tumor cell lines and one normal cell line to study the structural activity of ligands and iron complexes. The mechanism of ligand inhibiting cell cycle and its ability to promote apoptosis were analyzed.

2. Results and discussion

2.1. Synthesis and crystal structure description of C3

We have synthesized and characterized five iron chelator derived from 2,6-diacetylpyridine bis(acylhydrazones) to test the anticancer proliferative activity of this ligand. The preparation of the ligand (L1–L5) follows the previously reported scheme for synthesizing a 2,6-diacetylpyridine bis(acylhydrazones) with a high–yield Schiff base condensation reaction (Scheme 1). These compounds are slightly soluble in water but have greater solubility in polar solvents such as acetonitrile, DMF and DMSO. The Fe(III) complexes were produced by the coordination of the ligand with Fe(III) chloride in an ethanol solution (Scheme 1). Identification of crystal structure of Fe(III) complex crystals filtered from methanol solution by X–ray single crystal diffractometer.

The structure refinement and crystal data of **C3** were revealed in Table 1, and the angles (deg) and bond lengths (Å) of **C3** were showed in Table S1–2. The system and space group of **C3** were monoclinic and P21/c, respectively. The coordination mode of L3 is the predicted quinquidentate N3O2 (Fig. 1). The Fe(III) metal center of **C3** is coordinated by three N atoms (N1, N2 and N4), two O atoms (O1 and O2) and two Cl atoms (Cl1 and Cl2), which forms a deformation of decapicosecond configuration (Fig. 1). The Fe–N distances (2.168 Å–2.209 Å) were shorter than the Fe–Cl distances (2.3457 Å and 2.3696 Å) and longer than Fe–O distances (2.070 Å and 2.104 Å). The bond length and bond angle of **C3** are similar to the reported Fe complexes [39,40].

Table 1
Structure refinement and crystal data of **C3**.

Identification code	**C3**
Empirical formula	$C_{23}H_{23}Cl_3FeN_5O_5$
Formula weight	611.66
Temperature/K	296.15
Crystal system	Monoclinic
Space group	$P2_1/c$
a, b, c/Å	7.4241(11), 14.997(2), 23.220(4)
α, β, γ/°	90, 92.439(3), 90
Volume/Å^3	2582.8(7)
Z	4
Index ranges	$-8 \le h \le 4$, $-17 \le k \le 17$, $-26 \le l \le 27$
Reflections collected	12,936
Independent reflections	4531 [R_{int} = 0.0558, R_{sigma} = 0.0690]
Data/restraints/parameters	4531/0/341
Goodness–of–fit on F^2	0.972
Final R indexes [$I \ge 2\sigma$ (I)]	R_1 = 0.0482, wR_2 = 0.1029
Final R indexes [all data]	R_1 = 0.0901, wR_2 = 0.1144
CCDC NO.	1876580

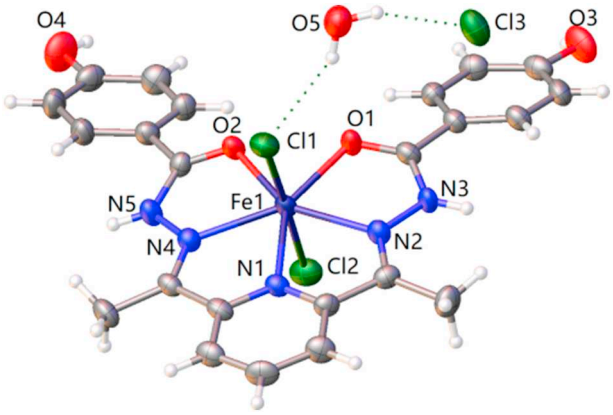

Fig. 1. Molecular structure of Fe(III) complex showing the environment about the Fe(III) atom.

2.2. Anticancer properties of ligands and Fe complexes

We studied the anti–cancer properties of 2,6-diacetylpyridine bis (acylhydrazones) analogues and their corresponding Fe(III) complexes on several typical cell lines: MCF–7 (human breast adenocarcinoma cell line), NCI–H460 Cells (human large cell carcinoma), A549 (adenocarcinomic human alveolar basal epithelial cell line) and LO–2 (human normal liver cell line). The results in Table 2 show that both ligands and Fe(III) complexes have low cytotoxicity to normal cells (LO–2). This study revealed that L2, L4 and L5 have a potential anticancer proliferation activity (IC_{50}: 9.2–3.1 μM; Table 2). After incubation with

Table 2
IC_{50} values of ligands and Fe complexes toward cell lines for 72 h.

	IC_{50} ± SD (μM)			
	MCF–7	A549	NCI–H460	LO–2
L1	43.5 ± 0.5	42.3 ± 0.5	54.7 ± 0.3	> 100
L2	8.4 ± 0.1	9.2 ± 0.1	7.4 ± 0.1	62.4 ± 0.9
L3	43.5 ± 0.3	42.1 ± 0.4	44.2 ± 0.2	> 100
L4	3.6 ± 0.1	3.3 ± 0.1	5.7 ± 0.1	67.8 ± 0.4
L5	4.4 ± 0.1	3.1 ± 0.1	7.1 ± 0.2	78.4 ± 0.9
C1	> 100	> 100	> 100	> 100
C2	53.3 ± 0.3	58.3 ± 0.5	63.2 ± 0.6	> 100
C3	61.6 ± 0.4	72.1 ± 0.8	73.1 ± 0.7	> 100
C4	40.8 ± 0.3	33.1 ± 0.5	48.4 ± 0.5	> 100
C5	50.6 ± 0.6	52.9 ± 0.7	54.3 ± 0.5	> 100
Cisplatin	3.25 ± 0.32	4.73 ± 0.21	3.21 ± 0.19	8.92 ± 0.43
$FeCl_3$	> 100	> 100	> 100	> 100

Table 3
Comparison of the RR inhibitory potency of ligands and Fe complexes in A549 cells.

Ligand	IC_{50} of ligands	IC_{50} of Fe complexes	p value
L1	64.6 ± 5.6	> 100	–
L2	22.6 ± 3.5	97.4 ± 11.4	$p < 0.001$
L3	87.4 ± 8.3	> 100	–
L4	18.9 ± 2.5	88.9 ± 8.1	$p < 0.001$
L5	15.6 ± 2.1	76.3 ± 6.9	$p < 0.001$
Triapine	6.9 ± 0.5	53.8 ± 5.4	$p < 0.001$

A549 cells for 72 h, the antitumor activity of L4 (IC_{50}: 3.3 ± 0.1 μM) was similar to L5 (IC_{50}: 3.1 ± 0.1 μM), higher than L1 (IC_{50}: 42.3 ± 0.5 μM) and L3 (IC_{50}: 42.1 ± 0.4 μM), which indicates that the modification of the methyl or methoxide group on the acylhydrazone ligand helps to increase antitumor activity. All five Fe(III) complexes (**C1–C5**) and $FeCl_3$ do not have significant antitumor activity and cytotoxicity against normal cells (IC_{50} > 50 μM; Table 2). The Fe(III) complexes (**C1–C5**) has a significant ($p < 0.001$) decreased anticancer proliferation activity compared to the corresponding ligand (L1–L5), which indicates that the anticancer mechanism of the acylhydrazone ligands may be caused by the disruption of iron metabolism in the cell, which causes the cell to stop proliferating. Therefore, we carried on an in–depth and systematic study of the anticancer mechanisms with acylhydrazone ligands and Fe(III) complexes.

2.3. Iron chelators significantly inhibit ribonucleotide reductase activity

In order to determine whether coordination with iron (III) has a difference in cytotoxicity and inhibition of RR, ^{3}H–Cytidine DNA incorporation operated to determine in A549 cells after 4 h of acylhydrazone ligands and Fe(III) complexes incubation. As revealed in Table 3, the RR inhibitory potential agrees with the same trends as observed in the cytotoxicity tests. The inhibited RR activity of L2, L4 and L5 enhanced 2.9, 3.4 and 4.1 times, respectively, relative to L1. The RR inhibition data show significantly decrease after the formation of complexes. These results demonstrate that the anticancer mechanisms of the 2,6-diacetylpyridine bis(acylhydrazones) analogues is likely to dependent on RR inhibition. We selected a ligand (L5) with the best anti–tumor proliferative activity and inhibition of RR activity and the corresponding iron complex (**C5**) for further study.

2.4. Iron chelators significantly inhibit cell division

The CFDA SE (Carboxyfluorescein diacetate, succinimidyl ester) entering the cell is catalytically decomposed into CFSE by esterase, which spontaneously and irreversibly binds to the Lysine residue or other amino group of the intracellular protein and labels these proteins [41,42]. Since the fluorescence of CFDA SE–labeled cells is very uniform and stable, the fluorescence of each progeny cell is reduced by half, so that cells without division and dividing cells can be detected by flow cytometry [43]. Fig. 2A shows that the control cells underwent three divisions within 24 h, and the proportions of generation 0–3 are 15.3%, 49.9%, 28.0% and 6.73%, respectively. The ratio of L5–treated generation 0 increased to 76.0%, while the ratio of generation 1–3 has significantly decreased (Fig. 2A and D). The cell division activity of **C5** treated is the same as that of the control cells.

2.5. Iron chelators significantly inhibit cell cycle

The inhibition of RR activity leads to the inability of DNA to synthesize normally, further affecting the cell cycle [44–46]. The regulation of cell cycle will be useful for in-depth understanding of biological growth, development and controlling tumor growth, et al. [47,48]. PI was used to stain the A549 cell line to assess the effect of the 2,6-diacetylpyridine bis(acylhydrazones) analogue and Fe complexes cell cycle (Fig. 3). The percentage of cells in the S phase treated with control, L5 and **C5** was 42.81%, 78.69%, 45.72% after 24 h incubation, respectively (Fig. 3). These results indicate that L5 can induce cell cycle arrest in S phase through a decrease in cell cycle progression in G1 and G2 phases. Furthermore, the Fe(III) complex (**C5**) had no significant effect on the cell cycle, which is consistent with the cytotoxicity data.

2.6. The expression of cell cycle related protein affected by iron chelator

Cell cycle arrest may be regulated by cell cycle–associated proteins, such as CDK 2, CDK 4, Cyclin A and Cyclin E [49,50]. To examine the effect of 2,6-diacetylpyridine bis(acylhydrazones) analogues and Fe complexes on proteins in A549 cells, Western blot experiments were performed and the results are shown in Fig. 4. After exposure of A549 cells to 20 μM of L5 for 24 h, the expression of CDK 2, CDK 4, Cyclin A and Cyclin E were markedly ($p < 0.001$) decreased by 0.59, 0.69, 0.72 and 0.35–fold relative to the control, respectively (Fig. 4). Fe(III) complex (**C5**) have no significant effect on the expression of CDK 2, CDK 4, Cyclin A and Cyclin E, which was consistent with cell cycle results.

2.7. The expression of ferritin and transferrin receptor–1 affected by iron chelator

Previous studies have demonstrated that iron chelators can affect the iron metabolism of cells and promote the dissipation of iron in cells [51]. Western blotting was used to detect the ability of L5 to affect transferrin receptor–1 (TfR1) and ferritin expression compared with the control. DFO as a positive control significantly increased (2.4 times the control) expression level of TfR1 and decreased the expression level of ferritin (0.59 times of control). After exposure of A549 cells to 20 μM of L5 for 24 h, the expression of TfR1 were markedly ($p < 0.001$) increased by 2.4–fold relative to the control, while the expression of ferritin was significantly ($p < 0.001$) decreased by 0.61–fold relative to the control (Fig. 4). However, the expression levels of the two proteins **C5** (TfR1 and ferritin) had no significant effect (Fig. 5).

2.8. Intracellular ROS measurements

Previous studies have revealed that iron complexes can catalyze the production of reactive oxygen species (ROS) by hydrogen peroxide when entering cells which will cause apoptosis [50,52]. To detect the effects of 2,6-diacetylpyridine bis(acylhydrazones) analogues and Fe complexes on intracellular ROS in A549 cells, fluorescent 2,7–dichlorofluorescein (DCF) probe and flow cytometry were employed (Fig. 6). The DCF fluorescence intensity of cells seeded with L5 and **C5** showed no peak shift to the right compared to control cells, indicating no change in ROS levels in these cells (Fig. 6). This results indicate that the anticancer mechanism of 2,6-diacetylpyridine bis(acylhydrazones) analogues may be not combined with intracellular iron ions to catalyze the hydrogen peroxide to product ROS.

2.9. Cell apoptosis assay

The main pathway by which various antitumor drugs induce cell death is apoptosis. Studying the occurrence and regulation of apoptosis is of great significance for improving the efficacy of drugs and developing new anti–tumor drugs [53]. Whether 2,6-diacetylpyridine bis(acylhydrazones) analogues and Fe complexes promote apoptosis are further verified by Annexin V–FITC/PI staining. Quantification of the result showed A549 cell apoptosis (early apoptosis and late apoptosis) of 7.15% for control, 17.09% for L5 and 13.05% for **C5**, respectively, which shows that L5 and **C5** did not significantly ($p > 0.05$) promote A549 cells apoptosis. These results indicate that the anticancer mechanism of 2,6-diacetylpyridine bis(acylhydrazones) analogues may be not promote apoptosis (Fig. 7).

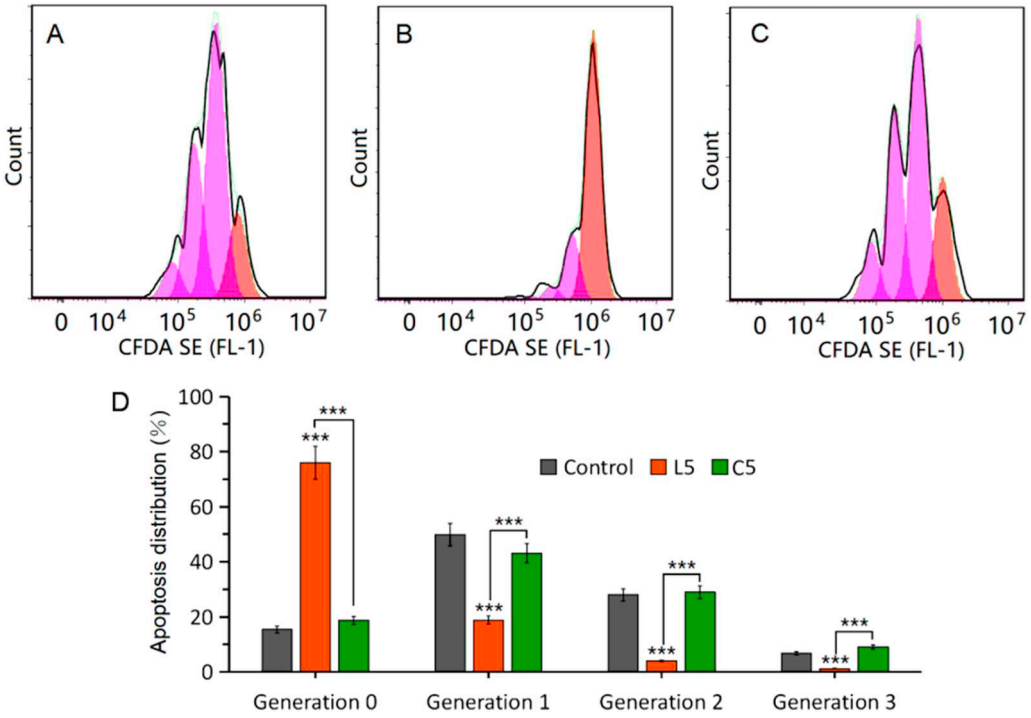

Fig. 2. The proliferation of A549 cells was inhibited by the treatment of control (A); 20 μM of L5 (B) and 20 μM of **C5** (C) for 24 h. (D) Comparison of the proliferation of A549 cells treated with L5 and **C5**. ***$p < 0.05$.

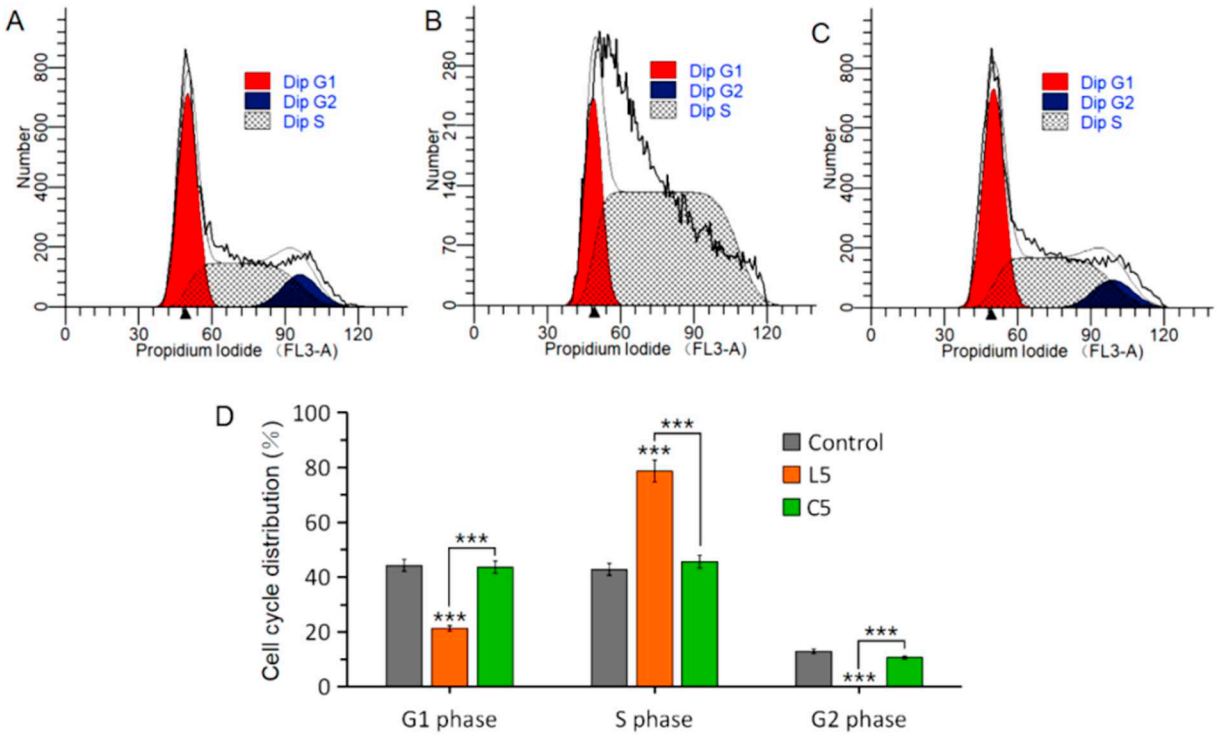

Fig. 3. Effect of the cell cycle of A549 treated with control (A); 20 μM of L5 (B) and 20 μM of C5 (C) for 24 h. (D) Comparison of cell cycle distributions of A549 cells treated with L5 and **C5**. ***$p < 0.05$.

3. Conclusion

Herein, we prepared five 2,6-diacetylpyridine bis(acylhydrazones) analogues Schiff base ligands and five Fe complexes. The structure of **C3** was verified by X–ray diffraction. The results indicated that the ligands have higher anti–tumor proliferative activity relative to the corresponding Fe(III) complex. Further studies have shown that ligands and complexes have different anti–tumor mechanisms. 2,6-Diacetylpyridine bis(acylhydrazones) (L5) has a significant effect on RR activity, cell proliferation, and cell cycle, while Fe(III) complexes has

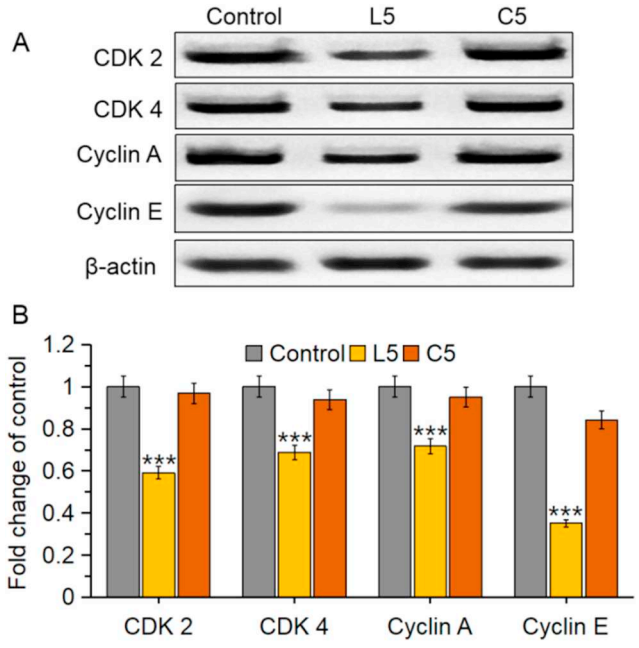

Fig. 4. (A) Western blot analysis of CDK 2, CDK 4, Cyclin A and Cyclin E levels after 20 μM of L5 and **C5** treatment. β–actin was used as internal control. (B) Quantitative analysis of the expression of CDK 2, CDK 4, Cyclin A and Cyclin E. The percentage values are those relative to the control. ***p < 0.001.

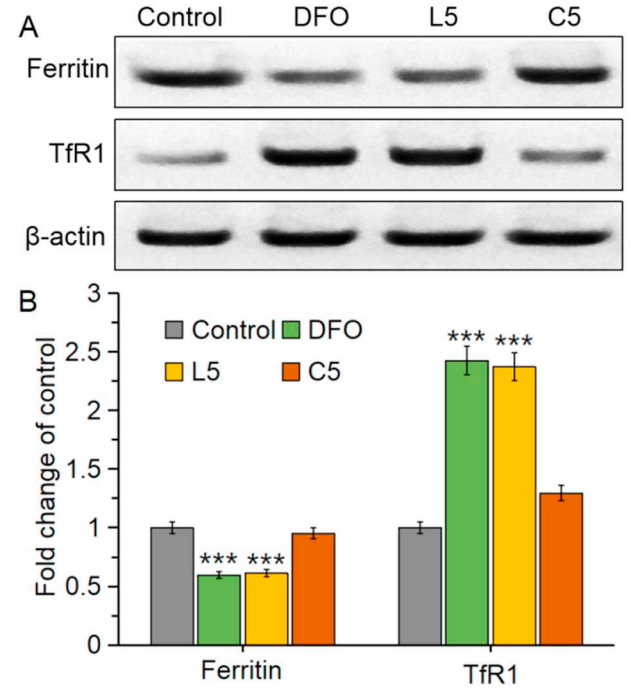

Fig. 5. (A) Western blot analysis of TfR1 (transferrin receptor–1) and ferritin levels after 20 μM of L5 and **C5** treatment. β–Actin was used as internal control. (B) Quantitative analysis of the expression of TfR1 and ferritin. The percentage values are those relative to the control. ***p < 0.001.

not. When A549 cells exposed to the ligand, the expression of transferrin receptor–1 is significantly increased, while the expression of ferritin is significantly reduced. Interestingly, this phenomenon disappears with the Fe(III) complex treatment. Neither ligand nor iron complex can increase intracellular reactive oxygen species (ROS) level and promote apoptosis.

4. Materials and methods

4.1. Material

2,6-Diacetylpyridine, benzoyl hydrazine, isoniazid, p–toluic hydrazide, 4–hydroxybenzhydrazide, p–anisohydrazide and other chemicals were analytical grade supplied by Innochem Company (Shanghai, China). Distilled water and the solvent used in the study did not need to be future purification. The cell lines operated in the experiment were purchased from Chinese academy of sciences.

4.2. Synthesis and characterization of ligands and Fe(III) complexes

4.2.1. Synthesis and characterization of ligands

Ligands (L1–L5) were prepared with the previous method [54,55]. 2,6-diacetylpyridine was dissolved in ethanol solution (10 mL), with stirring, followed by 5 drops of acetic acid glacial and acylhydrazones (One mole equivalent) refluxed for 4 h. The precipitate was separated with filter paper and washed by ice–cold ethanol. A vacuum desiccator was performed for drying the product.

2,6-Diacetylpyridine bis(benzoylhydrazone) (L1): yield 74%. *Anal. Calcd* for $C_{23}H_{21}N_5O_2$: C, 69.16; H, 5.30; O, 8.01. Found: C, 69.38; H, 5.37; O, 8.22. ESI–MS *m/z* (%) 400.17 $[M + H]^+$. ^1H NMR (600 MHz, DMSO–d_6) δ 11.47 (s, 2H), 8.96 (d, J = 5.8 Hz, 6H), 8.19 (d, J = 7.7 Hz, 1H), 8.14 (dd, J = 11.6, 5.3 Hz, 4H), 8.08 (d, J = 5.5 Hz, 2H), 8.01 (dd, J = 4.5, 1.8 Hz, 2H), 2.59 (s, 6H).

2,6-diacEtylpyridine bis(benzoylhydrazone) (L2): yield 71%. *Anal. Calcd* for $C_{21}H_{19}N_7O_2$: C, 62.83; H, 4.77; O, 7.97. Found: C, 62.76; H, 4.83; O, 7.91. ESI–MS *m/z* (%) 402.16 $[M + H]^+$. ^1H NMR (600 MHz, DMSO–d_6) δ 11.08 (s, 2H), 8.05 (s, 1H), 7.98 (s, 6H), 7.60 (t, J = 7.5 Hz, 2H), 7.53 (t, J = 7.5 Hz, 4H), 2.55 (s, 6H).

2,6-Diacetylpyridine bis(benzoylhydrazone) (L3): yield 76%. *Anal. Calcd* for $C_{23}H_{21}N_5O_4$: C, 64.03; H, 4.91; O, 14.83. Found: C, 64.01; H, 4.97; O, 14.80. ESI–MS *m/z* (%) 432.16 $[M + H]^+$. ^1H NMR (600 MHz, DMSO–d_6) δ 10.67 (s, 2H), 10.18 (s, 2H), 8.08 (s, 2H), 7.93 (d, J = 8.4 Hz, 1H), 7.81 (d, J = 8.3 Hz, 4H), 6.91–6.86 (m, 4H), 2.53 (s, 6H).

2,6-Diacetylpyridine bis(benzoylhydrazone) (L4): yield 74%. *Anal. Calcd* for $C_{25}H_{25}N_5O_2$: C, 70.24; H, 5.89; O, 7.49. Found: C, 70.29; H, 5.82; O, 7.41; O, 8.22. ESI–MS *m/z* (%) 428.20 $[M + H]^+$. ^1H NMR (600 MHz, DMSO–d_6) δ 10.83 (s, 2H), 8.14 (s, 2H), 7.94 (s, 1H), 7.83 (t, J = 9.5 Hz, 4H), 7.32 (dd, J = 24.5, 7.9 Hz, 4H), 2.54 (s, 6H), 2.40 (s, 6H).

2,6-Diacetylpyridine bis(benzoylhydrazone) (L5): yield 74%. *Anal. Calcd* for $C_{25}H_{25}N_5O_4$: C, 65.35; H, 5.48; O, 13.93. Found: C, 65.31; H, 5.43; O, 13.98. ESI–MS *m/z* (%) 460.19 $[M + H]^+$. ^1H NMR (600 MHz, DMSO–d_6) δ 10.77 (s, 2H), 8.23–8.03 (m, 3H), 7.91 (d, J = 8.9 Hz, 4H), 7.07 (d, J = 8.5 Hz, 4H), 3.85 (d, J = 0.9 Hz, 6H), 2.54 (s, 6H).

4.2.2. Synthesis and characterization of Fe(III) complexes

Fe(III) complexes (**C1–C5**) were prepared with the previous methods [39]. Ligands were dissolved in the methanol solution (10 mL), with stirring, followed by one mole equivalent of $FeCl_3$. Single crystals of Fe(III) complexes were prepared by the solvent evaporation method. The crystals were separated and rinsed by cold ethanol. A vacuum desiccator was used for drying the Fe(III) complexes.

$[Fe(L1)Cl_2]Cl$ (C1): yield 78%. *Anal. Calcd* for $C_{23}H_{21}Cl_3FeN_5O_2$: C, 49.18; H, 3.77; O, 5.70. Found: C, 49.12; H, 3.71; O, 5.74. ESI–MS *m/z* (%) 525.04 $[M–Cl]^+$.

$[Fe(L2)Cl_2]Cl$ (C2): yield 77%. *Anal. Calcd* for $C_{21}H_{19}Cl_3FeN_7O_2$: C, 44.75; H, 3.40; O, 5.68. Found: C, 44.71; H, 3.42; O, 5.63. ESI–MS *m/z* (%) 527.03 $[M–Cl]^+$.

$[Fe(L3)Cl_2]Cl$ (C3): yield 81%. *Anal. Calcd* for $C_{22}H_{20}Cl_3FeN_5O_4$: C, 45.51; H, 3.47; O, 11.02. Found: C, 45.45; H, 3.42; O, 11.07. ESI–MS *m/z* (%) 557.03 $[M–Cl]^+$.

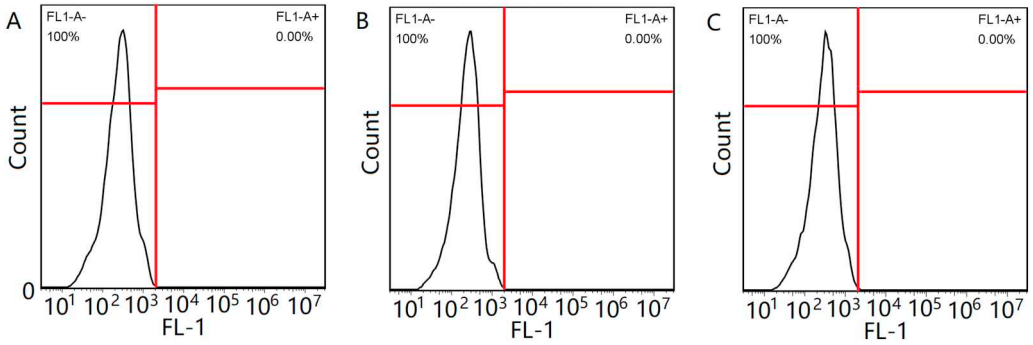

Fig. 6. Intracellular production of ROS of A549 cells by the treatment of control (A); 20 μM of L5 (B) and 20 μM of **C5** (C) for 24 h.

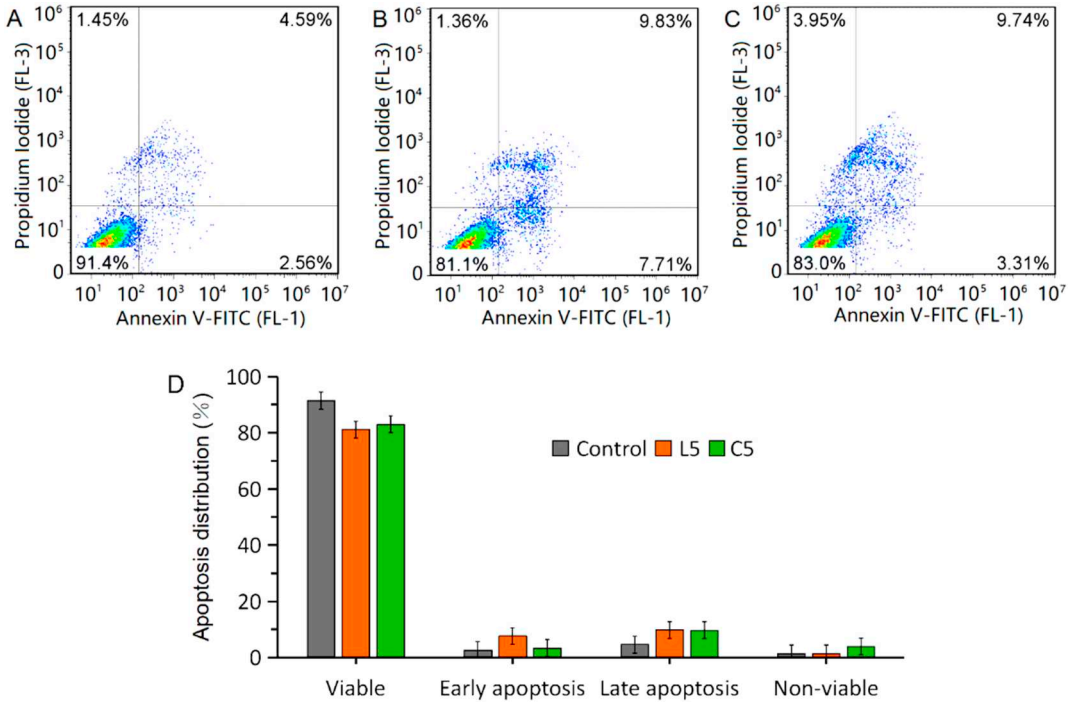

Fig. 7. Representative dot plots of Annexin V and PI double staining on the A549 cells by the treatment of control (A); 20 μM of L5 (B) and 20 μM of **C5** (C) for 24 h. (D) Comparison of apoptosis distributions of A549 cells treated with L5 and **C5**.

[Fe(L4)Cl_2] Cl (C4): yield 74%. *Anal. Calcd* for $C_{25}H_{25}Cl_3FeN_5O_2$: C, 50.92; H, 4.27; O, 5.43. Found: C, 50.88; H, 4.22; O, 5.47. ESI–MS *m/z* (%) 553.07 $[M–Cl]^+$.

[Fe(L5)Cl_2] Cl (C5): yield 73%. *Anal. Calcd* for $C_{25}H_{25}Cl_3FeN_5O_4$: C, 48.30; H, 4.05; O, 10.29. Found: C, 48.35; H, 4.03; O, 10.22. ESI–MS *m/z* (%) 585.06 $[M–Cl]^+$.

4.3. Determination of structure of C3

A Bruker SMART Apex II CCD diffractometer was conducting at 296.15 K for achieving X–ray crystallographic data, with Mo–Kα (λ = 0.71073 Å) radiation source. Empirical absorption corrections (multiscan) and data reduction were predicted by Oxford Diffraction CrysAlisPro software. The structure of **C3** was solved by direct methods with Olex2 and refined against F^2 by full-matrix least–squares methods with Olex2 software [56]. H atoms were controlled at geometrically positions by a riding model, while Non-hydrogen atoms were anisotropic. Structure diagrams of Fe(III) complexes were described by Olex2 software. The Crystal Data of Fe(III) complexes were displayed in Table 1. The bond lengths and angles of complexes were showed in Table S1.

4.4. Cytotoxicity assay (MTT)

In an incubator (ThermoFisher), the cell lines were cultivated at 5% CO_2/95% air, 37 °C. The cell cytotoxicity was examined by MTT (3-(4,5-dimethyl-2-thiazolyl)-2,5-diphenyl-2-H-tetrazolium bromide) assay. Fe(III) complexes and ligands were dissolved in stock solutions (10 mM) of DMSO (Dimethyl Sulphoxide). Different concentration of compounds was diluted by cell culture medium to ensure DMSO concentration < 0.1% which will not influence cell proliferation. A 96 well plate was cultured with 100 μl medium (5×10^4 cells), and incubated for 12 h at 37 °C, 5% CO_2/95%, followed by different concentrations (100, 50, 25, 10, 1, 0 μM) Fe(III) complexes and ligands for 72 h, then 20 μL of MTT (5 mg/mL) was added to it at 37 °C, 5% CO_2 for 4 h. The living cells' optical density (OD) was characterized at 570 nm wavelength, after adding 100ul of DMSO. IC_{50} (half maximal inhibitory concentration) values were provided by the nonlinear multipurpose curve–fitting program GraphPad Prism.

4.5. Ribonucleotide reductase inhibition

The test substances were seeded to exponentially growing A549 cells (5×10^6) for 4 h. At 37 °C. ^{3}H–cytidine (0.3125 μCi, 5 nM) was

used for A549 cells for 1 h. The cells were collected and rinsed with PBS, and dissolved in a lysis buffer containing 50 mM Tris (pH 8.0), 10 mM EDTA, and 0.5% sodium lauryl sarcosinate, frozen at −20 °C. Cell lysates were incubated in 20 units of RNase for 1 h using standard procedures, and then DNA was extracted after treatment it with 150 μg of Proteinase K for 24 h. The precipitate was precipitated with ethanol, dissolved in water, and the DNA content and radioactivity were measured.

4.6. Cell division analysis

Proliferative capacity was determined with 5,6–carboxyfluorescein diacetate succinimidyl ester (CFSE) (Beyotime, China) dilution assay [57]. The cells labeled with CFSE and incubated on 6-well plate for 12 h were collected and rinsed with PBS (phosphate buffer, pH = 7.4) for 3 times after treated with 20 μM of L5 or **C5** for 24 h. The fluorescence intensity was detected with an FCMScan flow cytometer (BD Accuri C6) and solved with FlowJo software.

4.7. Cell cycle analysis

At 37 °C, 5% CO_2/95%, 5 mL of A549 cells (1×10^5 cells/mL) were seeded and incubated for 12 h in 70 mm petri dish. The cells were collected and rinsed with PBS (phosphate buffer, pH = 7.4) for 3 times after treated with 20 μM of L5 or **C5** for 24 h. Then cells were fixed with 75% ethanol at −20 °C for 12 h and washed with cold PBS. The samples were incubated with RNase (Ribonuclease) A (2.5 mg/mL) and stained by propidium iodide (50 mg/mL) for 0.5 h. 10,000 events were recorded for each sample and operated by flow cytometry (FACScan, Becton Dickinson, USA). MFLT32 software was used for analyzing the data.

4.8. Western blot analysis

The 5 mL A549 cells (1×10^5 cells/mL) were incubated at 37 °C, 5% CO_2/95% for 24 h in 100 mm petri dish. Samples were collected after being fed with 20 μM of L5 or **C5** for 24 h and rinsed with cold PBS (phosphate buffer, pH = 7.4) for 3 times. The cells were disrupted in lysis buffer. The supernatant was separated by centrifugation at 10,000*g* for 0.25 h at 4 °C. The SDS–polyacrylamide gel electrophoresis was used for analyzing the samples, while the BCA assay kit (Beyotime, China) was used for recognizing the protein's concentration. After adding a polyvinylidene fluoride membrane to the ice bath for 3 h, the protein was stored in TBST buffer containing 5% skim milk at 25 °C for 1 h. At 4 °C, the membranes were seeded with primary antibodies overnight and rinsed with TBST (0.05% Tween 20, 20 mM Tris–HCl, 150 mM NaCl, pH 8.0) for 3 times. Secondary antibodies were used for incubating the membrane for 1 h at 25 °C and washed it again. The immunoreactivity was characterized by Amersham ECL Plus (Amersham) and the amount of proteins of each lane was revealed by β–actin.

4.9. Intracellular ROS measurements

Intracellular ROS generation was characterized by Flow Cytometer with the specification of the Reactive oxygen species assay kit (KeyGEN BioTECH, Nanjing). In serum free cell culture medium, 20 μM of L5 or **C5** was added to A549 cells for 0.5 h. The samples were incubated for 0.5 h at 37 °C with 2 μM H_2DCF–DA and rinsed with serum free medium for twice times. With excitation 488 nm and emission wavelength at 525 nm, the Flow Cytometer was applied to assay the samples, which were analyzed by FlowJo software.

4.10. Cell apoptosis assay

The A549 cell apoptotic events induced by L5 or **C5** were measured by PI staining and Annexin V with the manufacturer's suggestion for the Annexin V: FITC Apoptosis Detection Kit (Bection Dickinson). After 2 ml the cells (1×10^5 cells/mL) were seeded with 20 μM of L5 or **C5** for 24 h at 37 °C, 5% CO_2/95%, the samples were suspended in 100 μL Annexin V–binding buffer and followed by the adding of 5 μL each of Annexin V and PI. Next, the samples incubated at room temperature for 15 min was measured by flow cytometry analysis (BD Accuri C6). Apoptosis results were analyzed by FlowJo software. All tests were conducted at least three times.

4.11. Statistical analysis

All three experiments were conducted at least. The significance of differences was evaluated by Student's *t*-test. Data was revealed as mean ± SD with $p < 0.05$was needed.

Acknowledgements

This work was supported by National Natural Science Foundation of China (81571812), Priority Academic Program Development of Jiangsu Higher Education Institutions (1107047002), the Fundamental Research Funds for the Central Universities and Postgraduate Research & Practice Innovation Program of Jiangsu Province (KYCX17_0135). The research was also supported by the Scientific Research Foundation of Graduated School of Southeast University (YBJJ1787).

Conflict of interest

The authors declare that they have no conflict of interests.

Appendix A. Supplementary data

Supplementary data to this article can be found online at https://doi.org/10.1016/j.jinorgbio.2019.01.003.

References

[1] N.T.V. Le, D.R. Richardson, Blood 104 (2004) 2967–2975.
[2] J.M. Myers, Q. Cheng, W.E. Antholine, B. Kalyanaraman, A. Filipovska, E.S.J. Arnér, C.R. Myers, Free Radic. Biol. Med. 60 (2013) 183–194.
[3] C.R. Chitambar, W.E. Antholine, Antioxid. Redox Signal. 18 (2013) 956–972.
[4] A. Popović-Bijelić, C.R. Kowol, M.E.S. Lind, J. Luo, F. Himo, É.A. Enyedy, V.B. Arion, A. Gräslund, J. Inorg. Biochem. 105 (2011) 1422–1431.
[5] R.J. Martinie, E.J. Blaesi, C. Krebs, J.M. Bollinger Jr., A. Silakov, C.J. Pollock, J. Am. Chem. Soc. 139 (2017) 1950–1957.
[6] E.J. Blaesi, G.M. Palowitch, K. Hu, A.J. Kim, H.R. Rose, R. Alapati, M.G. Lougee, H.J. Kim, A.T. Taguchi, K.O. Tan, T.N. Laremore, R.G. Griffin, C. Krebs, M.L. Matthews, A. Silakov, J.J. Bollinger, B.D. Allen, A.K. Boal, Proc. Natl. Acad. Sci. U. S. A. 115 (2018) 10022–10027.
[7] G.I. Rozman, D. Lundin, M. Sahlin, M. Crona, G. Berggren, A. Hofer, B.M. Sjoberg, J. Biol. Chem. 293 (2018) 15889–15900.
[8] M. Sagawa, H. Ohguchi, T. Harada, M.K. Samur, Y.T. Tai, N.C. Munshi, M. Kizaki, T. Hideshima, K.C. Anderson, Clin. Cancer Res. 23 (2017) 5225–5237.
[9] M.F. Zaltariov, M. Hammerstad, H.J. Arabshahi, K. Jovanovic, K.W. Richter, M. Cazacu, S. Shova, M. Balan, N.H. Andersen, S. Radulovic, J. Reynisson, K.K. Andersson, V.B. Arion, Inorg. Chem. 56 (2017) 3532–3549.
[10] A. Tebbi, O. Guittet, K. Tuphile, A. Cabrie, M. Lepoivre, J. Biol. Chem. 209 (2015) 14077–14090.
[11] M.C. Chen, B. Zhou, K. Zhang, Y.C. Yuan, F. Un, S. Hu, C.M. Chou, C.H. Chen, J. Wu, Y. Wang, X. Liu, D.L. Smith, H. Li, Z. Liu, C.D. Warden, L. Su, L.H. Malkas, Y.M. Chung, M.C. Hu, Y. Yen, Mol. Pharmacol. 87 (2015) 996–1005.
[12] K. Iwamoto, K. Nakashiro, H. Tanaka, N. Tokuzen, H. Hamakawa, Int. J. Oncol. 46 (2015) 1971–1977.
[13] P. Han, Z.R. Lin, L.H. Xu, Q. Zhong, X.F. Zhu, F.Y. Liang, Q. Cai, X.M. Huang, M.S. Zeng, Mol. Med. Rep. 12 (2015) 401–409.
[14] T. Tachibana, J. Kanda, S. Machida, T. Saito, M. Tanaka, Y. Najima, S. Koyama, T. Miyazaki, E. Yamamoto, M. Takeuchi, S. Morita, Y. Kanda, H. Kanamori, S. Okamoto, Int. J. Hematol. 107 (2018) 578–585.
[15] K. Lam, C. Chan, S.J. Done, M.N. Levine, R.M. Reilly, Nucl. Med. Biol. 42 (2015) 78–84.
[16] M. de Lima, J. McMannis, A. Gee, K. Komanduri, D. Couriel, B.S. Andersson, C. Hosing, I. Khouri, R. Jones, R. Champlin, S. Karandish, T. Sadeghi, T. Peled, F. Grynspan, Y. Daniely, A. Nagler, E.J. Shpall, Bone Marrow Transplant. 41 (2008) 771–778.
[17] L. Dai, Z. Lin, J. Qiao, Y. Chen, E.K. Flemington, Z. Qin, Oncogene 36 (2017) 5068–5074.

[18] G. Graser-Loescher, A. Schoenhuber, C. Ciglenec, S. Eberl, G. Krupitza, R.M. Mader, S.S. Jadav, V. Jayaprakash, M. Fritzer-Szekeres, T. Szekeres, P. Saiko, Food Chem. Toxicol. 108 (2017) 53–62.
[19] J. Matsumoto, B.F. Kiesel, R.A. Parise, J. Guo, S. Taylor, M. Huang, J.L. Eiseman, S.P. Ivy, C. Kunos, E. Chu, J.H. Beumer, J. Pharm. Biomed. Anal. 146 (2017) 154–160.
[20] N.S. Moorthy, N.M. Cerqueira, M.J. Ramos, P.A. Fernandes, Mini-Rev. Med. Chem. 13 (2013) 1862–1872.
[21] S. Becchi, A. Buson, J. Foot, W. Jarolimek, B.W. Balleine, Br. J. Pharmacol. 174 (2017) 2302–2317.
[22] Y. Wang, T.Y. Wong, W. Chan, Chem. Res. Toxicol. 29 (2016) 1560–1564.
[23] C. Lazzarini, K. Haranahalli, R. Rieger, H.K. Ananthula, P.B. Desai, A. Ashbaugh, M.J. Linke, M.T. Cushion, B. Ruzsicska, J. Haley, I. Ojima, P.M. Del, Antimicrob. Agents Chemother. 62 (2018) e00156-18.
[24] B. Cobeljic, M. Milenkovic, A. Pevec, I. Turel, M. Vujcic, B. Janovic, N. Gligorijevic, D. Sladic, S. Radulovic, K. Jovanovic, K. Andelkovic, J. Biol. Inorg. Chem. 21 (2016) 145–162.
[25] S.A. Carvalho, L.O. Feitosa, M. Soares, T.E. Costa, M.G. Henriques, K. Salomao, S.L. de Castro, M. Kaiser, R. Brun, J.L. Wardell, S.M. Wardell, G.H. Trossini, A.D. Andricopulo, S.E. Da, C.A. Fraga, Eur. J. Med. Chem. 54 (2012) 512–521.
[26] A.E. Kummerle, M. Schmitt, S.V. Cardozo, C. Lugnier, P. Villa, A.B. Lopes, N.C. Romeiro, H. Justiniano, M.A. Martins, C.A. Fraga, J.J. Bourguignon, E.J. Barreiro, J. Med. Chem. 55 (2012) 7525–7545.
[27] C. Zhu, Y. Liu, L. Hu, M. Yang, Z.G. He, J. Biol. Chem. 293 (2018) 16741–16750.
[28] M.C. Schechter, D. Bizune, M. Kagei, M. Machaidze, D.P. Holland, A. Oladele, Y.F. Wang, P.A. Rebolledo, S.M. Ray, R.R. Kempker, Clin. Infect. Dis. 65 (2017) 1862–1871.
[29] J.F. Gallo, J. Pinhata, V. Simonsen, V. Galesi, L. Ferrazoli, R.S. Oliveira, Clin. Microbiol. Infect. 24 (2018) 889–895.
[30] T.J. Nagu, S. Aboud, M.I. Matee, M.J. Maeurer, W.W. Fawzi, F. Mugusi, J. Antimicrob. Chemother. 72 (2017) 876–881.
[31] D. Anthwal, R.K. Gupta, M. Bhalla, S. Bhatnagar, J.S. Tyagi, S. Haldar, J. Clin. Microbiol. 55 (2017) 1755–1766.
[32] G. Satta, A.A. Witney, R.J. Shorten, M. Karlikowska, M. Lipman, T.D. McHugh, BMC Med. 14 (2016) 117.
[33] C. Stefani, G. Punnia-Moorthy, D.B. Lovejoy, P.J. Jansson, D.S. Kalinowski, P.C. Sharpe, P.V. Bernhardt, D.R. Richardson, J. Med. Chem. 54 (2011) 6936–6948.
[34] Z. Li, L. Wu, T. Zhang, Z. Huang, G. Qiu, Z. Zhou, L. Jin, Dalton Trans. 43 (2014) 7554–7560.
[35] R. Freitas, N.M. Cordeiro, P.R. Carvalho, M.A. Alves, I.A. Guedes, T.S. Valerio, L.E. Dardenne, L.M. Lima, E.J. Barreiro, P.D. Fernandes, C. Fraga, Chem. Biol. Drug Des. 91 (2018) 391–397.
[36] Y. Zheng, J. Ren, Y. Wu, X. Meng, Y. Zhao, C. Wu, Bioconjug. Chem. 28 (2017) 2620–2626.
[37] A.P. Jacomini, M. Silva, R. Silva, D.S. Goncalves, H. Volpato, E.A. Basso, F.R. Paula, C.V. Nakamura, M.H. Sarragiotto, F.A. Rosa, Eur. J. Med. Chem. 124 (2016) 340–349.
[38] D.A. Rodrigues, G.A. Ferreira-Silva, A.C. Ferreira, R.A. Fernandes, J.K. Kwee, C.M. Sant'Anna, M. Ionta, C.A. Fraga, J. Med. Chem. 59 (2016) 655–670.
[39] J. Qi, Y. Gou, Y. Zhang, K. Yang, S. Chen, L. Liu, X. Wu, T. Wang, W. Zhang, F. Yang, J. Med. Chem. 59 (2016) 7497–7511.
[40] P.J. Hill, L.R. Doyle, A.D. Crawford, W.K. Myers, A.E. Ashley, J. Am. Chem. Soc. 138 (2016) 13521–13524.
[41] N. Jbeily, R.A. Claus, K. Dahlke, U. Neugebauer, M. Bauer, F.A. Gonnert, J. Biophotonics 7 (2014) 369–375.
[42] S. Urbani, R. Caporale, L. Lombardini, A. Bosi, R. Saccardi, Cytotherapy 8 (2006) 243–253.
[43] T. Luzyanina, J. Cupovic, B. Ludewig, G. Bocharov, J. Math. Biol. 60 (2014) 1547–1583.
[44] A. Chabes, B. Stillman, Proc. Natl. Acad. Sci. U. S. A. 104 (2007) 1183–1188.
[45] Y. Kaplan, M. Kupiec, Curr. Genet. 51 (2007) 123–140.
[46] A. Jarry, L. Charrier, C. Bou-Hanna, M.C. Devilder, V. Crussaire, M.G. Denis, G. Vallette, C.L. Laboisse, Cancer Res. 64 (2004) 4227–4234.
[47] A.S. Krall, H.R. Christofk, Nature 546 (2017) 357–358.
[48] Z. Merhi, A.J. Polotsky, A.P. Bradford, E. Buyuk, J. Chosich, T. Phang, S. Jindal, N. Santoro, Reprod. Sci. 22 (2015) 1220–1228.
[49] J. Qi, Y. Zheng, K. Qian, L. Tian, G. Zhang, Z. Cheng, Y. Wang, J. Inorg. Biochem. 177 (2017) 110–117.
[50] J. Qi, Q. Yao, L. Tian, Y. Wang, Eur. J. Med. Chem. 158 (2018) 853–862.
[51] J. Qi, Q. Yao, K. Qian, L. Tian, Z. Cheng, Y. Wang, J. Inorg. Biochem. 186 (2018) 42–50.
[52] M. Zhu, J. Wang, J. Xie, L. Chen, X. Wei, X. Jiang, M. Bao, Y. Qiu, Q. Chen, W. Li, C. Jiang, X. Zhou, L. Jiang, P. Qiu, J. Wu, Eur. J. Med. Chem. 157 (2018) 1395–1405.
[53] G. Jaouen, A. Vessieres, S. Top, Chem. Soc. Rev. 44 (2015) 8802–8817.
[54] J. Qi, Q. Yao, K. Qian, L. Tian, Z. Cheng, D. Yang, Y. Wang, Eur. J. Med. Chem. 154 (2018) 91–100.
[55] J. Qi, K. Qian, L. Tian, Z. Cheng, Y. Wang, New J. Chem. 42 (2018) 10226–10233.
[56] O.V. Dolomanov, L.J. Bourhis, R.J. Gildea, J.A.K. Howard, H. Puschmann, J. Appl. Crystallogr. 42 (2009) 339–341.
[57] E.D. Hawkins, M. Hommel, M.L. Turner, F.L. Battye, J.F. Markham, P.D. Hodgkin, Nat. Protoc. 2 (2007) 2057–2067.